Inelastic chaotic scattering on a Bose-Einstein condensate

Stefan Hunn, Moritz Hiller, and Andreas Buchleitner
Physikalisches Institut, Albert-Ludwigs-Universität Freiburg, Hermann-Herder-Str. 3, 79104 Freiburg, Germany

Doron Cohen
Department of Physics, Ben-Gurion University, Beer-Sheva 84105, Israel

Tsampikos Kottos
Department of Physics, Wesleyan University, Middletown, Connecticut 06459, USA
(Dated: October 12, 2010)

We devise a microscopic scattering approach to probe the excitation spectrum of a Bose-Einstein condensate. We show that the experimentally accessible scattering cross section exhibits universal Ericson fluctuations, with characteristic properties rooted in the underlying classical field equations.

PACS numbers: 03.65.Nk, 05.45.Mt, 67.85.Hj

Introduction.— Bose-Einstein condensates (BEC) in optical lattices provide a versatile tool to address experimentally a variety of questions that emerge in diverse fields ranging from quantum information and many-body quantum phase transitions to solid-state transport and atomtronics. An important element of these studies is the development and implementation of methods which allow for an accurate measurement of the properties of the condensate. Among the most popular ones are time-of-flight and Bragg-spectroscopy [1–6] techniques which result in the destruction of the BEC, whereas only few works consider a scattering setup that leaves the condensate intact [7]. Specifically, the main focus of the present literature is on photon-atom scattering, while only very recently it was shown how to probe the Mott insulator to superfluid transition by matter-wave scattering on the condensate ground state [8]. However, excited states of the many-body problem are naturally populated in experiments which probe non-trivial BEC dynamics [9]. The rapidly emerging complexity of the many-body dynamics – which manifest, e.g., in dynamical instabilities [10] – is a direct manifestation of the complex underlying spectral structure, which is itself rooted in the – in general chaotic – classical limit of the Bose-Hubbard model (achieved in the limit of large particle numbers). It is therefore timely to explore possible experimental strategies to probe these spectral features, in a non-destructive manner. In our present contribution, we show how an inelastically scattered probe particle can reveal the state of a BEC target in the parameter regime of spectral chaos. Due to the inherent sensitivity of spectral cross sections under such conditions, a robust characterization requires a statistical approach, which can be further sharpened by semiclassical considerations.

Model.— The scattering setup that we have in mind is shown in Fig. 1: A probe particle with momentum k moves in a waveguide which is placed in the proximity of a BEC confined by an optical lattice. When the particle approaches the condensate, it interacts with the latter – much as the condensate particles between themselves – leading to an exchange of energy. The particle energy on output from the waveguide defines the scattering cross section. The dynamics of the process is generated by the Hamiltonian

$$H_{\rm tot} = H_{\rm TB} \otimes \hat{1} + \hat{1} \otimes H_{\rm BH} + H_{\rm int}\,, \tag{1}$$

where $\hat{1}$ denotes the identity operator. In (1), $H_{\rm BH}$ represents the BEC target's Bose-Hubbard-Hamiltonian [11]

$$H_{\rm BH} = \frac{U}{2}\sum_{i=1}^{L} \hat{n}_i(\hat{n}_i - 1) - k\sum_i \left[\hat{b}_i^\dagger \hat{b}_{i+1} + \text{h.c.}\right] \tag{2}$$

of N interacting bosons on an L-site optical lattice, with $\hat{b}_i^{(\dagger)}$ the bosonic annihilation (creation) operators, and $\hat{n}_i = \hat{b}_i^\dagger \hat{b}_i$ the particle number at site i. U and k parameterize the on-site interaction and the intra-site tunneling strength, respectively. In the macroscopic limit $N \to \infty$ ($U \cdot N$ fixed), the dynamics of the condensate is well described by mean-field theory, i.e. the discrete Gross-Pitaevskii equation. In this limit, the quantum operators $b_i^{(\dagger)}$ are replaced by L complex amplitudes $A_i^{(*)}$ of a single-particle field. The Hamiltonian (2) then reads

$$\mathcal{H}_{\rm GP}/N = \frac{UN}{2}\sum_{i=1}^{L} |A_i|^4 - k\sum_i \left[A_i^* A_{i+1} + \text{c.c.}\right]\,, \tag{3}$$

where the A_i are time-dependent, and obey the canonical equations $i\partial A_j/\partial t = \partial \mathcal{H}_{\rm GP}/\partial A_j^*$.

The waveguide in our scattering scheme is modeled by two semi-infinite tight-binding (TB) leads with hopping term J and lattice spacing $a = 1$. These two leads are coupled with strength J_0 to the central site $j = 0$, which is closest to the condensate. J_0 thus controls the effective coupling of the projectile-target interaction region to the asymptotically free states of the lead. The probe-particle

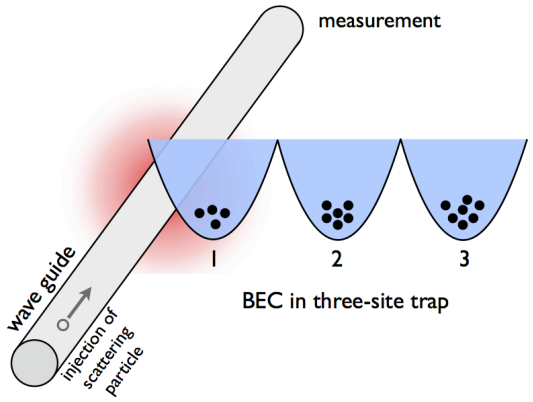

FIG. 1: (color online). Scattering setup: The probe particle is injected into a wave guide, and locally exchanges energy with a BEC confined by a three-site optical potential, in the contact region between wave guide and site one of the lattice. The inelastic scattering cross section measured on exit of the particle from the wave guide carries direct information on the state of the condensate.

Hamiltonian thus reads:

$$H_{\rm TB} = \Big[-J \sum_{j\neq -1,0} \hat{c}_j \hat{c}^\dagger_{j+1} - J_0 \sum_{j=-1,0} \hat{c}_j \hat{c}^\dagger_{j+1} \Big] + \text{h.c.}\,, \quad (4)$$

with $\hat{c}_j^{(\dagger)}$ the annihilation (creation) operators of the probe particle at site j of the TB lead. The particle's energy in the momentum eigenstate $|k_m\rangle$ is $\epsilon_m = -2J\cos(k_m)$, with corresponding velocity $v_m = 2J\sin(k_m)$ [12].

Finally, the probe-target interaction $H_{\rm int}$ is assumed to be of similar type (i.e. short range) as the bosonic inter-particle interaction in the condensate:

$$H_{\rm int} = \alpha \cdot \hat{c}_0^\dagger \hat{c}_0 \otimes \hat{n}_1\,. \quad (5)$$

For non-vanishing tunneling coupling k, $H_{\rm int}$ induces transitions between different eigenmodes of the condensate, what renders the scattering process inelastic. In this sense, $\alpha > 0$ controls the inelasticity. In the macroscopic limit, the interaction Hamiltonian becomes time-dependent, and is given by $\mathcal{H}_{\rm int} = \alpha N |A_1|^2 \cdot c_0^\dagger c_0$.

Scattering matrix.— Given the total Hamiltonian (1) and the asymptotic freedom of the probe particle, we can now define the scattering matrix of our problem, as the fundamental building block for our subsequent observations: For the condensate initially prepared in an energy eigenstate $|E_m\rangle$, and the probe particle injected with an energy ϵ_m, the total system energy is $\mathcal{E} = E_m + \epsilon_m$ [24]. The open channels (modes) of the scattering process are then determined by energy conservation and characterized by the kinetic energy $\epsilon_n = \mathcal{E} - E_n$ of the outgoing probe particle. The transmission block of the scattering matrix can be derived from the Green's function of a particle at site $j = 0$, with two semi-infinite leads attached,

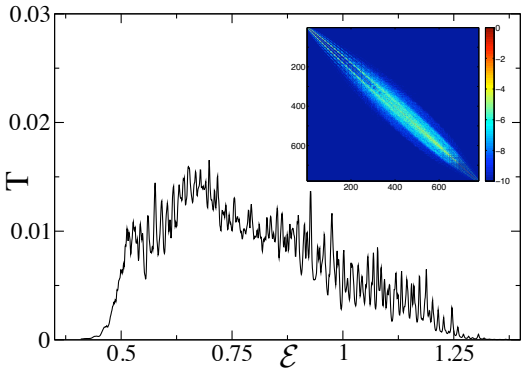

FIG. 2: (color online). Transmission T_m, averaged over the channels $m = 400 - 430$ in the chaotic regime, versus the total energy $\mathcal{E}$, for $\gamma = 0.001$, $N = 38$ bosons, and $\alpha = 5.0$. *Inset:* Logarithmically color-coded snapshot of the underlying interaction matrix Q.

and reads

$$[\hat{S}_T](\mathcal{E}) = \sqrt{\hat{v}}\,\frac{i\,\gamma}{(1-\gamma)[\mathcal{E} - \hat{H}_{BH}] - \alpha\hat{n}_1 + i\gamma v}\,\sqrt{\hat{v}}\,, \quad (6)$$

where $\gamma \equiv (J_0/J)^2$, and $\hat{v}$ is the velocity operator. In the eigenbasis of the BH Hamiltonian, both $\hat{H}_{BH}$ and $\hat{v}$ are diagonal matrices, while $\hat{n}_1$ is not. For $\gamma = 1$, Eq. (6) coincides with the S-matrix for inelastic electronic scattering in a 1D geometry derived in [13]. In our setup, $\gamma < 1$ can be regarded as a potential barrier that reduces the coupling between the leads and the scattering region (i.e. for $\gamma = 0$ the latter is isolated and the probe particle is perfectly reflected). As γ is increased from zero, one observes a crossover from a regime of well resolved, narrow resonances to a regime of overlapping resonances that we discuss below.

Chaotic scattering.— For $L > 2$ and intermediate values ($3 \lesssim u \lesssim 12$) of the control parameter $u = UN/2k$, the classical Hamiltonian $\mathcal{H}_{GP}$ (3) generates chaotic dynamics [14]. Quantum manifestations thereof were investigated in a series of publications with emphasis on the statistical properties of the energy spectra [15–18]. In our present contribution, we will investigate the properties of a probe particle scattering on a BEC that is described by the Hamiltonian (2). We focus on the parameter regime around $u = 5$, large filling factors of the lattice (i.e. $N \approx 50$ and $L = 3$), and a condensate initially prepared in an energy eigenstate $|E_m\rangle$ in the bulk of the spectrum, where the dynamics is predominantly chaotic [14].

How do the chaotic spectral properties of the BEC manifest in a scattering experiment as sketched in Fig. 1? The experimentally most easily accessible observable is the transmission $T_m(\mathcal{E}) = \sum_n |[S_T]_{nm}|^2$. It denotes the probability that a probe particle with incoming energy ϵ_m exits the scattering area in anyone of the outgoing chan-

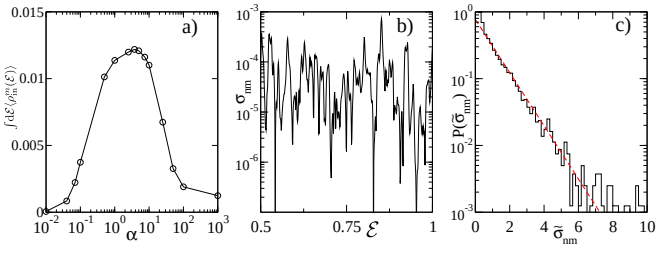

FIG. 3: (color online). *Left:* Integrated total inelastic cross section $\int \mathrm{d}\mathcal{E}\langle\rho^m_{\rm in}(\mathcal{E})\rangle$, for the same parameters as in Fig. 2, averaged over the channels $m = 400 - 430$ in the chaotic regime, versus the inelasticity parameter α. The integration runs over the entire energy axis. *Middle:* A representative inelastic cross section σ_{nm} versus the total energy $\mathcal{E}$, for the same parameters and $\alpha = 5$. *Right:* Histogram of the normalized inelastic cross section $P(\tilde{\sigma}_{nm})$, for fifteen different channels σ_{400m} $(m = 401 - 415)$ in the chaotic regime and identical parameter values. The data perfectly match the dashed straight line exponential fit.

nels ϵ_n. In Fig. 2, we show T_m versus the total energy $\mathcal{E}$, averaged over 30 incoming channels ϵ_m in the middle of the spectrum, i.e. in the chaotic regime: Strong fluctuations dominate the transmission signal. In the $\{|E_n\rangle\}$ basis, in which the scattering matrix is evaluated, the interaction operator $\hat{n}_1$ is the only non-diagonal quantity on the r.h.s. of (6) and thus represents the key ingredient. A closer inspection of the corresponding matrix $Q_{nm} \equiv \langle E_n|\hat{n}_1|E_m\rangle$ (see inset of Fig. 2) shows that for intermediate energies (in the center of the matrix), the matrix elements are erratically distributed, from what we conclude that S_T and thus all scattering quantities inherit their complexity from Q.

To gain insight in the role of the parameter α that controls the inelasticity induced by Q, we next consider the total inelastic scattering cross section

$$\rho^m_{\rm in}(\mathcal{E}) = 2\sum_{n\neq m} |[S_T(\mathcal{E})]_{nm}|^2 \,, \tag{7}$$

which essentially resembles T_m, except for the direct processes. For a given value of α, we integrate over the energy axis, to obtain robust results, unaffected by the sensitive energy dependence of $\rho^m_{\rm in}(\mathcal{E})$. Fig. 3a) shows that $\int \mathrm{d}\mathcal{E}\langle\rho^m_{\rm in}(\mathcal{E})\rangle_m$ takes its maximal value for intermediate values of the inelasticity parameter α, while it vanishes in the limit of small and large α. In the former case, the probe particle is directly transmitted, since (6) with $\alpha \approx 0$ becomes diagonal, while it is directly reflected in the latter case - as evident from (6) with $\alpha \gg 1$ in the denominator. Consequently, only for intermediate α-values can we infer information on the condensate from the probe particle's exit energy.

Ericson fluctuations.— Beyond total cross sections there is nontrivial dynamical information encoded in the *partial* inelastic cross sections $\sigma_{nm}(\mathcal{E}) \equiv |[S_T(\mathcal{E})]_{nm}|^2$, which quantifies the probability for a transition from a state E_m to a state E_n of the target (or, equivalently, from an energy ϵ_m to an energy ϵ_n of the probe particle). In Fig. 3b) we show $\sigma_{nm}(\mathcal{E})$, for the same parameter values as the transmission in Fig. 2. We observe much stronger fluctuations than for the total transmission, what is simply due to the fact that the latter imply an additional effective averaging over many scattering channels. As we will show now, this sensitive dependence on the energy is an unambiguous trait of (universal) Ericson fluctuations, hitherto only reported in the context of nuclear [19] and atomic physics [20, 21].

The rapid fluctuations of the cross section are due to interference effects between overlapping resonances: The scattering amplitudes $[S_T]_{nm}$ can be represented by a many-resonance Breit-Wigner formula, where each individual term in the sum is assumed to be a random variable. Then, due to the central limit theorem, one expects that both, real and imaginary part of $[S_T]_{nm}$ are Gaussian distributed random numbers with zero mean. This results in an exponential distribution [22] $P(\tilde{\sigma}_{nm}) = \exp[-\tilde{\sigma}_{nm}]$ of the normalized inelastic cross section $\tilde{\sigma}_{nm} = \sigma_{nm}/\bar{\sigma}_{nm}$, where $\bar{\sigma}_{nm}$ denotes the average inelastic cross section in the energy interval $\Delta\mathcal{E}$ (assumed to be small compared to classical energy scales). This expectation is clearly confirmed by our numerical data presented in Fig. 3c).

The central figure of merit to identify Ericson fluctuations is the energy autocorrelation function

$$C_{nm}(\varepsilon) = \int_{\Delta\mathcal{E}} \mathrm{d}\mathcal{E}(\sigma_{nm}(\mathcal{E}+\varepsilon) - \bar{\sigma}_{nm})(\sigma_{nm}(\mathcal{E}) - \bar{\sigma}_{nm}) \,. \tag{8}$$

A least-square fit of the numerically obtained autocorrelation as depicted in Fig. 4 shows that it perfectly matches a Lorentzian

$$C_{nm}(\varepsilon) \propto \frac{\Gamma^2}{\varepsilon^2 + \Gamma^2} \,, \tag{9}$$

with mean resonance width $\Gamma = 3.7{\cdot}10^{-3}/J$ [25], which is one order of magnitude larger than the mean level spacing $\Delta \approx 5{\cdot}10^{-4}/J$, directly extracted from our numerical data. This is in perfect agreement with Ericson's scenario of overlapping resonances, and can be underpinned by a semiclassical picture [23]:

The autocorrelation (9) can be interpreted as the squared Fourier transform of the survival probability $P(t)$ of the probe particle to stay a given time t in the scattering region, i.e. on the TB site $j = 0$, hence with $P(t) = |c_0(t)|^2$. That latter quantity is evaluated by direct solution of the classical evolution equations derived from (3, 5) (with initial conditions $P(0) = 1$ and the GP system prepared at an energy corresponding to E_m), and exhibits an exponential decay $P(t) \propto e^{-\beta t}$. β thus determines the width of the (classical) autocorrelation

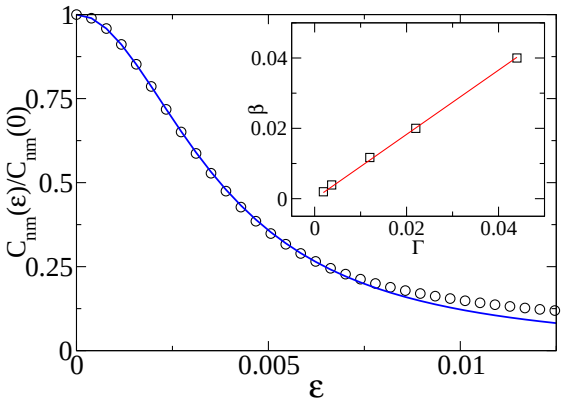

FIG. 4: (color online). Autocorrelation function $C_{nm}(\epsilon)$ (black ○) calculated from the inelastic scattering signal shown in Fig. 3b). The curve nicely matches a Lorentzian fit (blue). *Inset:* Semiclassical decay constant β versus the mean resonance width Γ (black □). The data points correspond to different values of the coupling constant γ. The semiclassical result is obtained after averaging over several initial conditions in the chaotic regime. The predicted correspondence ($\beta = \Gamma$) is confirmed by the fit $\beta = 0.92 \cdot \Gamma$ (red).

function $C_{\rm clas}(\varepsilon)$, by virtue of

$$C_{\rm clas}(\varepsilon) = \left| \int dt \; P(t) \exp(i\varepsilon t) \right|^2 , \qquad (10)$$

which implies an average over all outgoing probe energies ϵ_n. The inset of Fig. 4 demonstrates a perfect match of this semiclassically extracted quantity β with the width Γ of the autocorrelation extracted from the quantum mechanical cross section, and thus provides an independent, semiclassical proof of the Ericson scenario in the present many-particle problem.

Conclusions.— In the light of recent BEC experiments, the proposed scattering setup represents an experimentally feasible way to non-destructively probe the condensate and accurately resolve its robust spectral features. Measurements of the partial inelastic cross section can identify an unambiguous and semiclassically rooted case of Ericson fluctuations, which, in contrast to compound nuclear reactions, is here under perfect control, through the accurate experimental control of the underlying many-body Hamiltonian.

We acknowledge financial support by DFG *Research Unit 760*, the US-Israel Binational Science Foundation (BSF), Jerusalem, Israel, and by a grant from AFOSR No. FA 9550-10-1-0433.

[1] J. Stenger, S. Inouye, A. P. Chikkatur, D. M. Stamper-Kurn, D. E. Pritchard, and W. Ketterle, Phys. Rev. Lett. **82**, 4569 (1999).
[2] T. Stoferle, H. Moritz, C. Schori, M. Kohl, and T. Esslinger, Phys. Rev. Lett. **92**, 130403 (2004).
[3] A. M. Rey, P. B. Blakie, G. Pupillo, C. J. Williams, and C. W. Clark, Phys. Rev. A **72**, 023407 (2005).
[4] W. Chen, D. Meiser, and P. Meystre, Phys. Rev. A **75**, 023812 (2007).
[5] J. Larson, B. Damski, G. Morigi, and M. Lewenstein, Phys. Rev. Lett. **100**, 050401 (2008).
[6] S. Rist, C. Menotti, and G. Morigi, Phys. Rev. A **81**, 013404 (2010).
[7] I. B. Mekhov, C. Maschler, and H. Ritsch, Nature Phys. **3**, 319 (2007).
[8] S. N. Sanders, F. Mintert, and E. J. Heller, Phys. Rev. Lett. **105**, 035301 (2010).
[9] M. Albiez, R. Gati, J. Folling, S. Hunsmann, M. Cristiani, and M. K. Oberthaler, Phys. Rev. Lett. **95**, 010402 (2005).
[10] O. Morsch and M. Oberthaler, Rev. Mod. Phys. **78**, 180 (2006).
[11] D. Jaksch, C. Bruder, J. I. Cirac, C. W. Gardiner, and P. Zoller, Phys. Rev. Lett. **81**, 3108 (1998).
[12] S. Datta, *Electronic Transport in Mesoscopic Systems* (Cambridge University Press, 1995).
[13] S. Bandopadhyay and D. Cohen, Phys. Rev. B **77**, 155438 (2008).
[14] M. Hiller, T. Kottos, and T. Geisel, Phys. Rev. A **79**, 023621 (2009).
[15] L. Bernstein, J. C. Eilbeck, and A. C. Scott, Nonlinearity **3**, 293 (1990).
[16] L. Cruzeiro-Hansson, H. Feddersen, R. Flesch, P. L. Christiansen, M. Salerno, and A. C. Scott, Phys. Rev. B **42**, 522 (1990).
[17] R. Franzosi and V. Penna, Phys. Rev. E **67**, 046227 (2003).
[18] A. Buchleitner and A. R. Kolovsky, Phys. Rev. Lett. **91**, 253002 (2003).
[19] T. Ericson, Phys. Rev. Lett. **5**, 430 (1960).
[20] G. Stania and H. Walther, Phys. Rev. Lett. **95**, 194101 (2005).
[21] J. Madroñero and A. Buchleitner, Phys. Rev. Lett. **95**, 263601 (2005).
[22] T. Ericson and T. Mayer-Kuckuk, Annu. Rev. Nucl. Sci. **16**, 183 (1966).
[23] R. Blümel and U. Smilansky, Phys. Rev. Lett. **60**, 477 (1988).
[24] In our calculations we rescale the BH spectrum to lie within the bandwidth of the lead, and thereby avoid evanescent modes.
[25] Note that for a trimer prepared in the regular regime (i.e., $u \ll 1$ or $u \gg 1$), $C_{nm}(\varepsilon)$ shows significant deviations from a Lorentzian.